Surface modification of Ti6Al4V alloy scaffolds manufactured by electron beam melting

E Chudinova[1], M Surmeneva[1], AKoptyug[2], K Loza[3], O Prymak[3], M Epple[3], R Surmenev[1]

[1]Physical Materials Science and Composite Materials Centre, *National Research Tomsk Polytechnic University*, 30 Lenin Avenue, Tomsk 634050, Russian Federation
[2]Department of Mechanical Engineering and Quality Technology, SportsTech Research Centre, *Mid Sweden University*, Akademigatan 1, SE 831 25, Östersund, Sweden
[3]Inorganic Chemistry and Center for Nanointegration Duisburg-Essen (CeNIDE), *University of Duisburg-Essen,* Essen 45117, Germany

[1]E-mail: rsurmenev@mail.ru

Abstract. In this paper, the results of the surface functionalization of the Ti6Al4V alloy scaffolds with different structures for use as a material for medical implants are presented. Radio frequency magnetron sputtering was used to modify the surface of the porous structures by deposition of the biocompatible hydroxyapatite (HA) coating with the thickness of 860±50 nm. The surface morphology, elemental and phase composition of the HA-coated scaffolds were studied. According to energy-dispersive X-ray spectroscopy, the stoichiometric ratio of Ca/P for flat, orthorhombic and cubic scaffolds is 1.65, 1.60, 1.53, respectively, which is close to that of stoichiometric ratio for HA (Ca/P = 1.67). It was revealed that this method of deposition makes it possible to obtain the homogeneous crystalline coating both on the dense sample and in the case of scaffolds of complex geometry with different lattice cell structure.

1. Introduction

Additive manufacturing (AM), also called three-dimensional printing, allows fabricatingcomplex and multi-functional metal component from computer aided design models [1-3]. EBM is one of the powder-bed fusion AM technologies. This process shows great promise for making medical devices and industrial components through excellent shape control and strength to weight ratio [4-6]. This technology is suitable for producing near-net-shape small to medium volume metallic parts with complex geometries [7-10]. Additionally, the three-dimensional construct provides the necessary support for cells to proliferate and maintain their differentiated function, leading to superior bone regeneration and hard tissue replacement [11-13].

Titanium and its alloys (e.g., Ti6Al4V) are widely used as materials for the implants in orthopedics and dentistry. Porous Ti6Al4V scaffolds offer the following advantages over non-porous scaffolds: (i) a greater surface area for bone contact which enables vascularization, (ii) the possibility for bone ingrowth into the pores, improving mechanical interlocking between implant and bone, and (iii) reduced Young's modulus reducing the mismatch in the stiffness of bone and implant and thus

reducing the risk of stress shielding-induced bone loss [14-17]. Bioceramic layers based on calcium phosphate (CaP) have been applied as coatings on titanium-based implants, most often in the form of hydroxyapatite (HA), which has resulted in superior osteointegration. Titanium-based implants have been coated with HA due to its bioactivity, that is, ability to form a direct chemical bond with the surrounding bone [18-20].

The aim of this study was fabricating different cellular Ti6Al4V structures with a controllable interconnected porosity by EBM and to determine the effect of the deposited HA coatings onto mesh scaffolds.

2. Materials and methods

Dense (R1), porous (orthorhombic (R2) and cubic cell (R3)) scaffolds (figure 1) of Ti6Al4V alloy were fabricated by EBM system (Arcam® EBM, Mölndal, Sweden). Porous titanium alloy scaffolds are shaped as solid thin walled cups having outer diameter of 7 mm and overall height of 5 mm with the lattice inside. Dense scaffolds are cylindrical with the same outer dimensions. These structures were built layer-by-layer using the precursor Ti6Al4V (ELI) powder, with an average particle diameter of 70μm.Corresponding EBM equipment was described in detail earlier [21]. Briefly, the EBM system is a powder bed beam based AM system using electron beam to condition and melt metal powder layers. In each layer powder is melted according to the CAD model and chosen process parameter settings. Electron gun of ARCAM A2 machine used in this study works at 60 kV, 2 kW. Process parameter settings were chosen according to the manufacturer specification for Ti6Al4V with the temperature of material during manufacturing kept at 730 ^{o}C. All samples were carefully blasted in the standard ARCAM® powder recovery system, using the air flow containing the precursor powder.

Figure 1. Images of 3D macroporous scaffolds with the different type of cells.

The HA ($Ca_{10}(PO_4)_6(OH)_2$) coating layers were formed by radio-frequency (RF) magnetron sputtering deposition method on the Ti6Al4V alloy. A powder of HA was prepared using mechanochemical activation which was carried out in a planetary mill APF using two steel cylinders 750 mL in volume each. Steel balls with the mass of 1 kg (the mass ratio of balls to the mixture was 10:1.1) were loaded into each water-cooled cylinder. The frequency of the rotation of cylinders in the activator was 900 min^{-1}. The power of the mill allowed us to obtain the HA powder in the nanocrystalline state without subsequent thermal treatment [22]. After mechan-ochemical synthesis HA powder was used as a precursor to prepare a target for sputtering. The RF-power (400 W), argon gas pressure (working pressure 0.4 Pa, base pressure 10^{-4} Pa) and the distance between the target and substrate (40 mm) were kept constant in all experiments (deposition time was 8 hours). The thickness of HA film (860±50 nm) was determined using the Spectral ellipsometry complex Ellipse 1891 SAG.

The surface morphology was studied by scanning electron microscopy (SEM, ESEM Quanta 400 FEG).The energy-dispersive X-ray spectroscopy (EDX, Genesis 4000, SUTW-Si(Li) detector) was used for studying the elemental composition of the coating.

X-ray powder diffractometer with Cu Kα radiation (α=1.54 Å; 40 kV and 40 mA) was used to determine the internal structure and phase composition of the studied samples. The films were analyzed using Bragg-Brentano mode with Cu $K\alpha_1$ radiation at 2θ from 5 to 90° with a step size of 0.01°.

3. Results and discussion

Typical microscopy images of the samples fabricated by EBM before (figure 2, a-c) and after (figure 4, a-c, figure 5,a-c) deposition of the HA coatings and EDX spectra of the films, prepared on the Ti6Al4V alloy surface are shown in figure 2.It was found that the surface of the coated scaffold has a well-defined grain structure, the deposited HA layer is homogeneous without microcracks and any other visible defects.

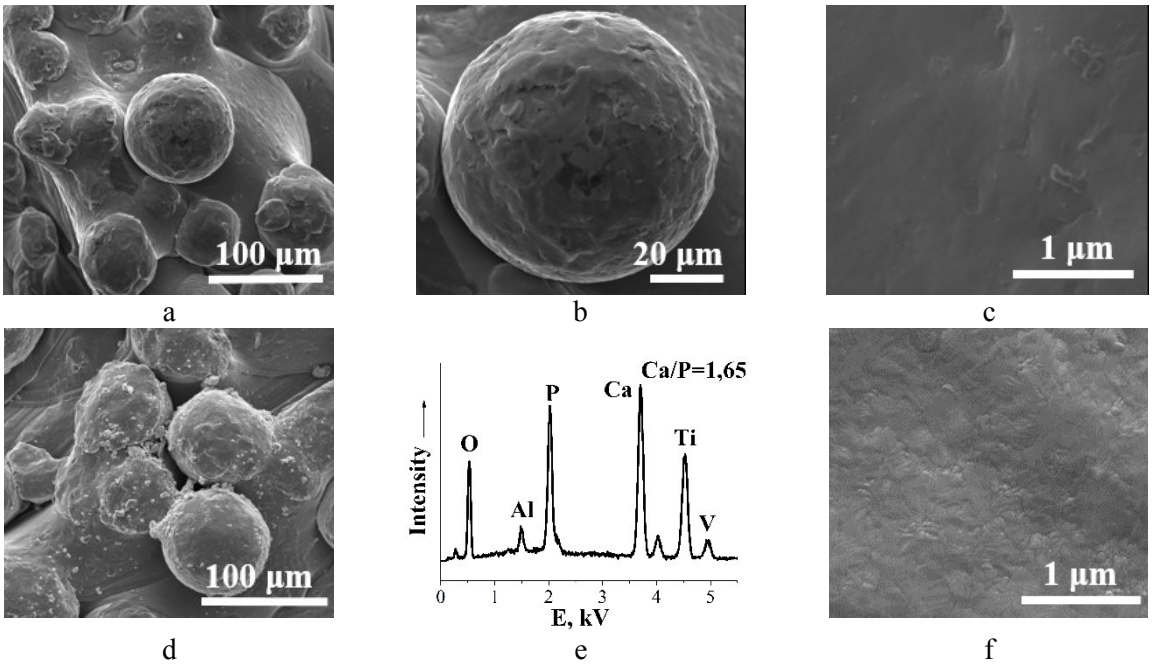

Figure 2. SEM images of scaffolds without treatment (a-c) and with coating based on HA(R1), EDX spectrum (e) of scaffolds with HA film.

According to EDX results, the stoichiometric ratio of Ca/P is 1.65, which is close to that for HA (Ca/P = 1.67).

The typical XRD-pattern of Ti6Al4V alloy prepared via additive manufacturing and HA coating fabricated on its surface via RF magnetron sputtering is shown in figure 3.

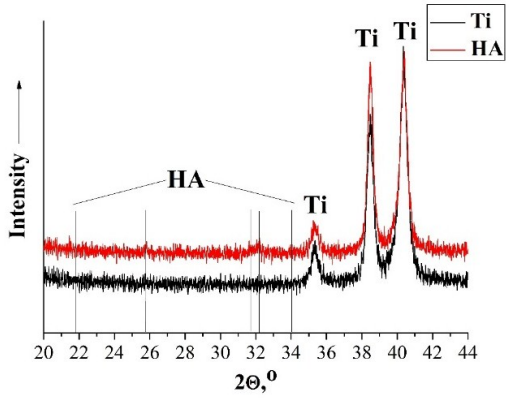

Figure 3. The typical XRD patterns of pure Ti and the composite of titanium–HA coating.

The peaks at 31.8º (211), 32.2º (112) and 34.0º (202) corresponded to the diffraction pattern of the HA with the hexagonal crystalline structure. In addition, low intensitypeaks at 22.9º (111) and 25.9º

(002) are also observed in the spectra. The most intensive peaks in the HA spectrum are at 31.8º (211) and 32.2º (112), which have also been observed elsewhere [23]. The deposition mechanism of HA in magnetron sputtering method can be described as the formation of amorphous calcium phosphate clusters, their conversion into HA nano-domains and crystallization of the grain domains with a preferential orientation along the HA [002] direction [24].

Figures 4a-4c and 5a-5c present SEM images of the HA-coated scaffolds with lattices R2 and R3, respectively. According to the SEM results (figure s4c and5c), a uniform grain structure is observed at the microlevel without defects and cracks.

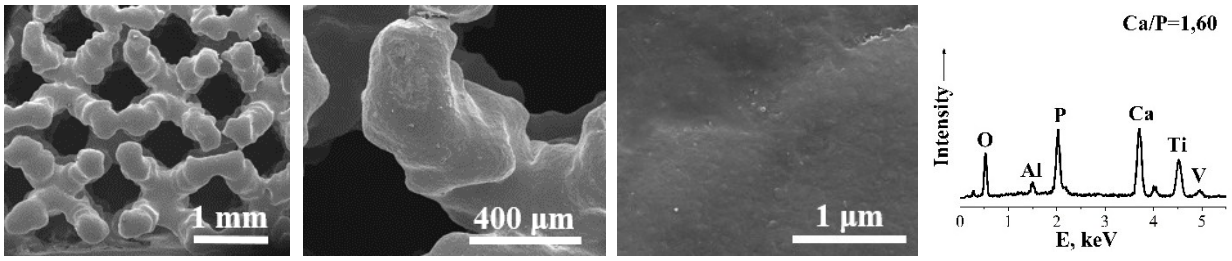

a b c d

Figure 4. SEM images (a-c) and EDX spectrum (d) of lattice cell R2 scaffold with HA coating.

A typical EDX spectrum of the HA-coated scaffolds is shown in figures 4d and 5d. The study shows the presence on the surface of Ca, P and O. The Ca/P ratio for the coating prepared on scaffolds with R2 and R3 lattice cell types were 1.60 and 1.53, respectively. According to the X-ray Photoelectron Spectroscopyresults presented in our previous study, the Ca/P ratio for nanocrystalline HA coatings deposited via the RF magnetron sputtering technique with comparable process parameters was reported in the range of 1.65–1.86 [11, 12].

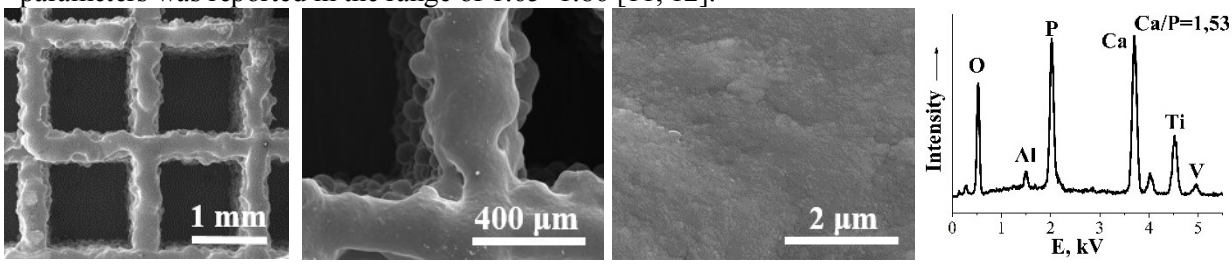

a b c d

Figure 5. SEM images (a-c) and EDX spectrum (d) of lattice cell scaffold R3 with HA coating.

Figure 6 presents a map of the elemental distribution within the formed HA layer for the porous samples with lattices of the type R2 and R3, respectively. In this case, a uniform distribution of the coating elements along the lattice cell surface is observed. Earlier [25], it was shown, that the method of RF magnetron deposition allows depositing biocompatible coating not only on the outer surface of a three-dimensional sample, but also on the inner layers of the scaffolds.

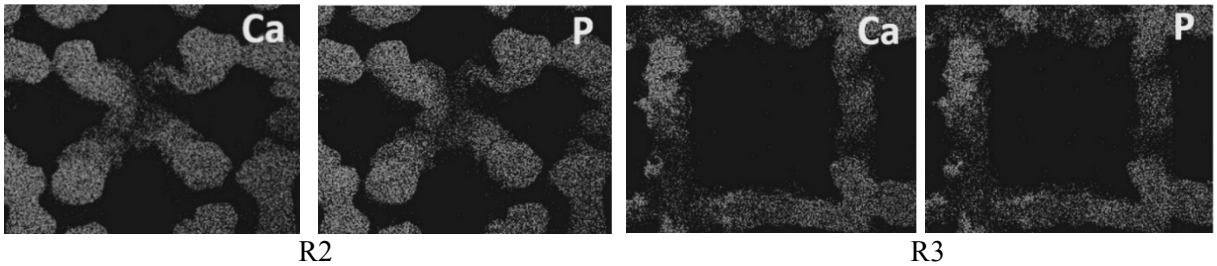

R2 R3

Figure 6. EDX element mapping data of deposited coatings.

4. Conclusions

RF magnetron sputtering was used to prepare an HA coating with the thickness of 860±50 nm on the surface of dense and reticulated bulk scaffolds prepared by EBM, powder bed electron beam- based AM technology. Investigation of the surface morphology of the scaffolds with different lattice cell types revealed that the grain structure is formed as a result of the deposition of the CaP layer. X-ray analysis showed the presence of an HA phase in the coating. Thus, RF magnetron sputtering is a promising method to deposit CaP layers on the Ti64 alloy scaffolds with the complex structure obtained by additive manufacturing.

Acknowledgments

This research was supported by the Russian Science Foundation grant No 15-13-00043 and the German-Russian Interdisciplinary Research Center (G-RISC, personal fellowship of Mrs E. Chudinova). The help of Ms. A. Ivanova in the measurement of the HA films thickness is acknowledged.

References

[1] Ngo TD, Kashani A, Imbalzano G, Nguyen KT and Hui D 2018 Additive manufacturing (3D printing): a review of materials, methods, applications and challenges *Compos.Part B-Eng.* **143** 172

[2] Bilgin M S, Baytaroğlu E N, Erdem A and Dilber E 2016 A review of computer-aided design/computer-aided manufacture techniques for removable denture fabrication *Eur. J. Dent.* **10/2** 286

[3] Dérand P, Rännar L E and Hirsch J M 2012 Imaging, virtual planning, design, and production of patient-specific implants and clinical validation in craniomaxillofacial surgery *Craniomaxillofac. Trauma and Reconstr.* **5/03** 137

[4] Baufeld B, Van der Biest O and Gault R 2010 Additive manufacturing of Ti–6Al–4V components by shaped metal deposition: microstructure and mechanical properties *Mater. Design* **31** S106

[5] Li S J, Xu Q S, Wang Z, Hou W T, Hao Y L, Yang R and Murr L E 2014 Influence of cell shape on mechanical properties of Ti–6Al–4V meshes fabricated by electron beam melting method *Actabiomaterialia* **10/10** 4537

[6] Wang P, Nai M L S, Tan X, Vastola G, Srinivasan R, Sin W J, Tor S B, Pei Q-X, Wei and J 2016 Recent progress of additive manufactured Ti-6Al-4V by electron beam melting In *Proceedings of the 2016 Annual International Solid Freeform Fabrication Symposium (SFF Symp 2016), Austin, TX, USA*.

[7] Wang P, Nai M L S, Sin W J, Lu S, Zhang B, Bai J, Song J and Wei J 2018 Realizing a full volume component by in-situ welding during electron beam melting process *Additive Manufact.* **22** 375

[8] Pham M T , Teo T J , Yeo S H , Wang P and Nai, M L S 2017 A 3-D Printed Ti-6Al-4V 3-DOF Compliant Parallel Mechanism for High Precision Manipulation *IEEE/ASME T. Mech.* **22/5** 2359

[9] Wang P, NaiM L S, Lu S, Bai J, Zhang B and Wei J 2017 Study of direct fabrication of a Ti-6Al-4V impeller on a wrought Ti-6Al-4V plate by electron beam melting *Jom* **69/12** 2738

[10] Wang P, Tan X, NaiM L S, Tor S B and Wei J 2016 Spatial and geometrical-based characterization of microstructure and microhardness for an electron beam melted Ti–6Al–4V component *Mater. Design* **95** 287

[11] Zhao S, Li S J, Hou W T, Hao Y L, Yang R and Misra R D K 2016 The influence of cell morphology on the compressive fatigue behavior of Ti-6Al-4V meshes fabricated by electron beam melting *J. Mech. Behav. Biomed.* **59** 251

[12] Arabnejad S, Johnston R B, Pura J A, Singh B, Tanzer M, Pasini D 2016 High-strength porous biomaterials for bone replacement: A strategy to assess the interplay between cell

morphology, mechanical properties, bone ingrowth and manufacturing constraints *Actabiomaterialia* **30** 345
[13] Tang D, Tare R S, Yang L Y, Williams D F, Ou K L, Oreffo R O 2016 Biofabrication of bone tissue: approaches, challenges and translation for bone regeneration *Biomater.* **83** 363
[14] Niinomi M 2008 Mechanical biocompatibilities of titanium alloys for biomedical applications *J. Mech. Behav. Biomed.* **1/1** 30
[15] Long M and Rack H J 1998 Titanium alloys in total joint replacement a materials science perspective *Biomater.* **19/18** 1621
[16] Wang P, Todai M and Nakano T 2018 ω-phase transformation and lattice modulation in biomedical β-phase Ti-Nb-Al alloys *J. All. Comp.* **766** 511
[17] Wang P, Wu L, Feng Y, Bai J, Zhang B, Song J and Guan S 2017 Microstructure and mechanical properties of a newly developed low Young's modulus Ti–15Zr–5Cr–2Al biomedical alloy *Mate. Sci. Eng. C* **72** 536
[18] Mróz W, Budner B, Syroka R, Niedzielski K, Golański G, Slósarczyk A, Schwarze D and Douglas T E 2015 In vivo implantation of porous titanium alloy implants coated with magnesium-doped octacalcium phosphate and hydroxyapatite thin films using pulsed laser deposition *J. Biomed. Mater. Res. B Appl. Biomater.* **103/1** 151
[19] Chambers B, Clair S F S and Froimson M I 2007 Hydroxyapatite-coated tapered cementless femoral components in total hip arthroplasty *J. Arthroplasty* **22/4** 71
[20] Xia L, Xie Y, Fang B, Wang X & Lin K 2018 In situ modulation of crystallinity and nano-structures to enhance the stability and osseointegration of hydroxyapatite coatings on Ti-6Al-4V implants *Chem. Eng. J.* **347** 711
[21] KlingvallEk, R 2016 *Surface properties of implants manufactured using electron beam melting*, Doctoral dissertation, Mid Sweden University.
[22] Chaikina M V, Pichugin V F, Surmeneva M A and Surmenev R A 2009 Mechanochemical synthesis of hydroxyapatite with substitutions for depositing the coatings on medical implants by means of high-frequency magnetron sputtering *Chem. Sust. Develop.* **17** 507
[23] Surmeneva M, Surmenev R, Nikonova Y, Selezneva I, Ivanova A, Putlyaev V, Prymak O, Epple M 2014 Fabrication, ultra-structure characterization and in vitro studies of RF magnetron sputter deposited nano-hydroxyapatite thin films for biomedical applications *Appl. Surf. Sci.* **317** 172
[24] López E O, Mello A, Sendão H, Costa L T , Rossi A L, Ospina R O and Rossi A M 2013 Growth of crystalline hydroxyapatite thin films at room temperature by tuning the energy of the RF-magnetron sputtering plasma *ACS Appl. Mater. Inter.* **5/19** 9435
[25] Chudinova E, Surmeneva M, Koptioug A, Scoglund P and Surmenev R 2016 Additive manufactured Ti6Al4V scaffolds with the RF-magnetron sputter deposited hydroxyapatite coating *J. Phys.: Conf. Ser.* **669/1** 012004